J Civil Struct Health Monit (2016) 6:839–850
DOI 10.1007/s13349-016-0203-6

ORIGINAL PAPER

Drive-by bridge damage monitoring using Bridge Displacement Profile Difference

Ahmed Elhattab[1] · **Nasim Uddin**[1] · **Eugene OBrien**[2]

Received: 29 July 2016 / Revised: 5 October 2016 / Accepted: 6 November 2016 / Published online: 14 November 2016

Abstract Recently, there has been a shift in emphasis in bridge monitoring from instrumentation of the bridge to instrumentation of a passing vehicle, known by "drive-by bridge inspection". This paper introduces a new method of identifying bridge damage using an instrumented truck; specifically using the truck acceleration histories to calculate changes in the "bridge displacement profile" which is shown to be sensitive to structural damage. The study includes three different bridges modeled as 1D FE beam elements and 2D FE plate elements. The simulation of the vehicle–bridge interaction is implemented in MATLAB. The truck is represented as a simple quarter car model crossing over a rough profile. The approach is also numerically tested for local damage in the bridge plate model. Finally, there is a study of sensitivity to signal noise, corrupted truck properties, initial conditions and transverse vehicle position.

Keywords Drive-by bridge inspection · Apparent profile · Bridge structural health monitoring · Indirect screening for bridge structures · Non-destructive evaluation

✉ Ahmed Elhattab
aahattab@uab.edu

Nasim Uddin
nuddin@uab.edu

Eugene OBrien
eugene.obrien@ucd.ie

[1] The University of Alabama at Birmingham, 1075 13th St S, Birmingham, AL 35205, USA

[2] School of Civil, Structural and Environmental Engineering, University College Dublin, Richview Newstead Block B, Belfield, Dublin 4, Ireland

1 Introduction

Bridges are amongst the most important elements of transport infrastructure, but are subject to continuous degradation due to environmental effects and may experience increases in traffic weight and volume over time. Therefore, they require continuous monitoring to ensure maintenance and hence their structural integrity. Visual inspection is considered as one of the most common methods to inspect bridges; however, a number of bridges collapsed just after they have been inspected [1]. Chupanit and Phromsorn [2] pointed to the importance of relying on other methods in the monitoring alongside the visual inspection, which fall under the structural health monitoring (SHM) techniques. For many years, monitoring has been based on instrumentation attached to the bridge, known by "sensor base monitoring". Many authors have investigated alternative techniques in this field [3–6]; however, the proposed techniques are costly which effectively limits the number of monitored bridges. Thus, there is a demand for an alternative method for quantifying the bridge damage without instrumenting the bridge, using indirect measurements from a passing vehicle. Yang et al. [7, 8] proposed a preliminary study in extracting the dynamic bridge properties from the acceleration history of a passing vehicle. The vehicle acceleration spectra are dominated by four main frequencies: the vehicle frequency, the driving speed frequency and two shifted bridge frequencies. The study also shows a drop in the shifted bridge frequencies for higher bridge damping ratios. Lin and Yang [9] experimentally assess the idea of extracting the fundamental bridge frequencies using a truck-trailer vehicle instrumented with accelerometers. They use the truck as a bridge exciter, while the trailer cart works as a receiver to the bridge response. The authors recommended installing the instrumentation to the cart suspension system, to avoid the

noise that may be transmitted by the vehicle engine. The truck-trailer passed over the bridge with different driving speeds and the cart acceleration was recorded. The results reveal a successful determination for the bridge fundamental frequency at driving speed lower than 40 km/h. In contrast, for higher driving speed the acceleration spectra are dominated by the cart frequency. Similar findings were observed when the test was made in the existence of an ongoing traffic, whereas the car response had been increased significantly comparing to the no-traffic case. Yang et al. [10] extended their study to investigate the variation of the bridge instantaneous frequency due to the presence of the inspection vehicle over the bridge. The authors show that the shift in the bridge frequency due to the inspection vehicle mass must be taken into account, especially if the vehicle mass is considerable comparing to the bridge or if resonance approached. This observation has been verified in field and lab by Chang et al. [11]. The authors provide an analytical formula for the shifted bridge frequency, function of the frequencies and the mass ratio between the vehicle and the bridge. This has been highlighted as an important consideration in the drive-by bridge inspection, where the shifted frequency may mask the effect of the damage.

The previous studies confirm the aspect of extracting the bridge dynamic properties using indirect measurements from a passing vehicle. Kim and Kawatani [12] extended this concept to identify the change in dynamic bridge properties due to structural damages. They introduce this concept as "drive-by bridge inspection". In their work, they used a scaled laboratory test to track the change in fundamental frequencies due to structural damage. The study shows that it is feasible to use the vehicle responses to track the change in the bridge frequency. McGetrick et al. [13] pointed out the importance of including the road roughness in the drive-by bridge inspection problems. First, they used a smooth profile for the theoretical vehicle–bridge interaction model. For this case, they successfully track the changes in the acceleration spectra due to the increase in the bridge damping ratio. On the other hand, for the rough profile, the acceleration spectra are dominated by the vehicle frequencies that mask the effect of changing the bridge damping on the spectrum. Keenahan et al. [14] solved this issue by introducing the concept of subtracted axle accelerations. In their work, they subtract the rear axle acceleration from the time-shifted front axle acceleration, i.e., when the rear axle reaches the position of the front axle, then apply fast Fourier transform (FFT) to the difference signal. The results show that the effect of the road roughness is largely removed from the power spectral density (PSD) curves. However, this study only considers damage represented as a change in damping ratio. Li et al. [15] switch to use an optimization process to extract the bridge frequency from passing vehicle responses. They used the generalized pattern search algorithm (GPSA) to search for the fundamental bridge frequency and the bridge stiffness. As a result, the approach has a potential to be used for bridge damage monitoring. The algorithm had been tested for a high signal-to-noise ratio (SNR = 5) and still identifies the damage with error margin of 3.3%. However, the authors did not include the road roughness effect which as shown before plays as a key parameter in the drive-by bridge inspection concept. Malekjafarian and OBrien [16] use the frequency domain decomposition (FDD) to process the vehicle responses instead of traditional FFT. They analyzed the acceleration signals of a two consecutive quarter car models. The vehicles are simulated crossing over the bridge in the presence of a road profile with low driving speed (2 m/s). The results show that the method successfully identifies both the bridge and the vehicle frequencies.

Toshinami et al. [17] have experimentally verified the feasibility of the drive-by bridge inspection approach, using an instrumented scaled model vehicle to cross over a scaled model bridge. The vehicle first crossed over a healthy bridge and over damaged bridges for different levels of damage. The approach was shown to be feasible in identifying the damage, but for moderate driving speeds only. For very low speeds the car did not excite the bridge enough to generate a significant response in the acceleration spectrum. For high speed, on the other hand, the spectrum resolution was not good enough to show the changes in power values.

Another trend in the drive-by bridge inspection is to identify the damage using bridge mode shapes. The mode shapes have the potential to localize the damage, using mode shapes discontinuity as a clue to the damage location. The feasibility of identifying discontinuities in curvature mode shapes has been proved by Pandey et al. [18] and Zhu and Law [19]. Zhang et al. [20] were the first to use an indirect bridge measurement to extract data correlated to the bridge mode shape. In the study, they used a specialized theoretical vehicle called "tapping vehicle", which is equipped with accelerometer and actuator to control the applied force on the bridge. The approach based on applying a predefined force to the bridge, then the vehicle response is used to construct the point impedance. The study shows that the amplitude of the point impedance spectra is proportional to the square of the mode shapes. In another field of research, Yang et al. [21] proposed an algorithm to extract bridge mode shapes from a passing vehicle measurement. They found that the instantaneous amplitude for the extracted bridge component response of specific mode is equal to the mode shape. The results show that the algorithm identifies the mode shapes with high resolution, since the vehicle used to pass over all bridge degrees of freedom; therefore, it has an indirect record for

each mode participation in the overall bridge response. Malekjafarian and OBrien [22] use short time frequency domain decomposition (STFDD) to estimate bridge modes shapes. In the study, the bridge is divided into segments, and the FDD is applied for the signals measured from two following axles. The authors investigated reducing the road roughness influence on the approach either by subtracting the acceleration history of the two axles with time gaps, or by increasing the bridge response through adding on going heavy traffic to the bridge. The results show that the approach estimates the bridge mode shapes with acceptable accuracy.

Previous studies focus on monitoring the change in the bridge fundamental frequency as a means of identifying the damage. Curadelli et al. [23] introduces the increase in structural damping as an alternative damage representation. The authors used wavelet transform to establish a procedure that identifies the undamped frequency and damping coefficient as a function of time. They experimentally investigate the procedure by testing a reinforced concrete beam, where the damage is imposed by applying a monotonic load on the beam. It has been shown the damping ratio and the damage severity are correlated, that as the damage increases the calculated damping coefficient increases too. McGetrick et al. [13] used this finding to study the feasibility of using an instrumented truck to extract information on bridge condition from changes in its damping value. The simulation of the vehicle–bridge interaction is performed in MATLAB [13], where the vehicle is represented as a quarter car and the damage as an increase in bridge damping value. They show that the approach works well in identifying the damping ratio change for smooth profiles, while for rough profiles the acceleration spectra are dominated by the vehicle excitation due to road roughness. González et al. [24] build an algorithm that identifies the bridge damping level using the axle acceleration history of an instrumented vehicle. The concept of the algorithm is to find the bridge damping value that minimizes the error in the back-calculated road profile under the front and rear axles of the vehicle.

Another group of authors investigated using the change in the bridge response as a mean of identifying the damage. McGetrick [25] and Gonzalez and Karoumi [26] use the Moving Force Identification algorithm (MFI), which is an inverse algorithm calculates the moving force history on the bridge, to track the changes in the force pattern due to structural damages. The approach shows to be very sensitive to detect the damage; on the other hand, it works for good profile roughness and under low level of signal noise. Zhang et al. [27] extended their work, by using the "tapping vehicle" to extract the operating deflection shape curvature (ODSC) as a bridge damage index. The operating deflection shape (ODS) is the square of the vehicle excitation frequency obtained by transforming the acceleration to the frequency domain using short time Fourier transform (STFT). While the ODSC is the square root for a normalized ODS [20]. The approach shows to detect local damages accurately considering a smooth intact structure. Miyamoto and Yabe [28, 29] made a novel achievement in the drive-by bridge inspection approach. In their work, they used a public bus instrumented with accelerometers at the frontal axle to monitor the structural anomaly parameters of the bridge. They estimate the bridge characteristic deflection using wave integrals obtained using Fourier transform. The noise influence is reduced by averaging different readings for the same bridge. The results were compared with signals measured from an accelerometer installed on the bridge and it shows a good match. The authors show that damage starts to take place when the calculated characteristic deflection exceeds specific limits.

OBrien and Keenahan [37] were the first to introduce the novel concept of using a traffic speed deflectometer (TSD) to identify bridge damage. The TSD is a specialist vehicle, designed for high-speed pavement stiffness measurement, which calculates the relative distances between the road surface and a horizontal beam on the truck. They use the TSD data to back figure the "apparent profile" (AP) defined here as the sum of the road profile and the bridge displacement history, as measured from the moving vehicle. The AP is shown to be sensitive to bridge damage as the vehicle crosses the bridge.

This paper introduces a new method for back-calculating the AP using a number of accelerometers in a non-specialist vehicle. The APs found from a number of sensors are then subtracted to calculate the "bridge displacement profile difference" (BDPD) which will be used as a damage indicator. The paper first shows the process of calculating the AP using the vehicle acceleration histories, then finding the BDPD for different damage extents. The approach is studied for 1D and 2D bridge models. The vehicle–bridge interaction (VBI) is solved using MATLAB. A sensitivity study is conducted to determine the effectiveness of the approach in the presence of different sources of measurement inaccuracy.

2 Vehicle and bridge properties

The vehicle is modeled as a quarter car with two degrees of freedom, the axle mass and body mass translations. The vehicle model is shown in Fig. 1, and its properties are based on the works of Cebon [30] and Harris et al. [31]. Three bridges are studied in this paper, each designed according to the AASHTO (1998) specifications. The bridge properties are shown in Table 2. The bridges are given an equal rectangular cross section to provide the

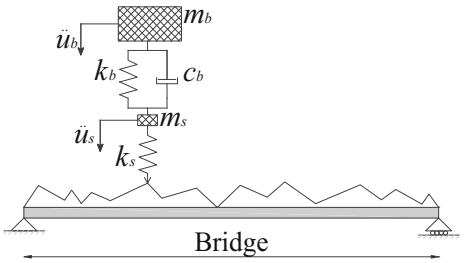

Fig. 1 Theoretical quarter car model

same dynamic bridge properties. The equivalent cross-sectional width and height are shown in Tables 1 and 2.

The bridges are first modeled with 1D Euler–Bernoulli finite beam elements with two degrees of freedom per node, vertical translation, and rotation. The bridges are also modeled using 2D plate bending finite elements. These elements have 3 degrees of freedom per node, vertical translation and rotations about the x and y axes. Figure 2 shows the plate bending element degrees of freedom (DOF).

The stiffness matrix of the plate bending element is derived using the method proposed by Logan [32], while the element mass matrix is derived based on the work of Zienkiewicz and Taylor [33] as follows:

$$[k_e] = \iint [B]^T [D][B] \mathrm{d}x\mathrm{d}y \tag{1}$$

$$[m_e] = \iint [N]^T \begin{bmatrix} \rho t & & \\ & \frac{\rho t^3}{12} & \\ & & \frac{\rho t^3}{12} \end{bmatrix} [N] \mathrm{d}x\mathrm{d}y, \tag{2}$$

where $[B]$ is the gradient matrix, $[D]$ is the constitutive matrix, $[N]$ is the element shape function, ρ is the material density and t is the element thickness.

3 Vehicle–bridge interaction modeling

The vehicle–bridge interaction problem is solved using the contact force concept adopted by Yang et al. [34] and González [35]. The approach is based on solving the vehicle and the bridge equations of motion separately and equating the contact forces between the vehicle and the bridge at each time step. The equations of motion for the vehicle and the bridge for time step i are:

$$[m_v]\{u_v\}_i + [c_v]\{\dot{u}_v\}_i + [k_v]\{u_v\}_i = \{f_v\}_i \tag{3}$$

$$[m_b]\{u_b\}_i + [c_b]\{\dot{u}_b\}_i + [k_b]\{u_b\}_i = \{f_b\}_i, \tag{4}$$

where $[m_v]$, $[c_v]$ and $[k_v]$ are the mass, damping and stiffness matrices for the vehicle, respectively, $\{u_v\}_i$, $\{\dot{u}_v\}_i$ and $\{u_v\}_i$ are the vehicle acceleration, velocity and displacement vectors, respectively, and $\{f_v\}_i$ is the applied force vector on the vehicle degrees of freedom. The components of this force vector, $\{f_v\}_i$ will have zero magnitude except for the axle mass degree of freedom, will equal f_{vc_i} which is as follows:

$$f_{vc_i} = (w_{b_i} + r_i)k_s, \tag{5}$$

where k_s is the suspension stiffness, w_{b_i} is the bridge displacement under the vehicle and r_i is the road profile under the vehicle. For the bridge,$[m_b]$, $[c_b]$ and $[k_b]$ are the mass, damming and stiffness matrices, respectively, $\{u_b\}_i$, $\{\dot{u}_b\}_i$ and $\{u_b\}_i$ are the bridge acceleration, velocity and displacement vectors, respectively and $\{f_b\}_i$ is the applied force vector on the bridge. The bridge force vector is calculated using the following equation:

$$\{f_b\}_i = \left(w - [m_v]\{u_v\}_i 1\right) \times \{N_b\}_i, \tag{6}$$

where w is the gravity weight of the vehicle, 1 is a row vector of the same order as the displacement vector containing unit values in all of its elements ($\langle 1 \rangle = [1, 1, 1, \ldots, 1]$). Here $\langle 1 \rangle$ is used to sum the products of the accelerations and the masses. $\{N_b\}_i$ is element shape function that distributes the load to the element degrees of freedom at the ith step. For the Euler–Bernoulli beam element, the Hermite cubic interpolation function is defined for each time step i according to the load location on the bridge. The shape function will have non-zero values if the vehicle is on the element, and will be zero otherwise. The same thing applies for the plate bending elements, except that the shape function is as introduced by Logan [32].

Table 1 Properties of quarter car model

Property	Unit	Symbol	Quarter car model
Body mass	kg	m_b	17,300
Axle mass	kg	m_s	700
Body stiffness	N/m	k_b	4×10^5
Body damping	N s/m	c_b	10×10^3
Suspension stiffness	N/m	k_s	1.75×10^6
Body mass frequency of vibration	Hz	f_{bounce}	0.69
Axle mass frequency of vibration	Hz	f_{axle}	8.8

Table 2 Bridges properties

Span (m)	Width (m)	High (m)	First natural frequency (Hz)	2nd moment of area around horizontal axis (m^4)	Section area (m^2)
10	4.04	0.51	8.75	0.0434	2.04
20	2.75	0.87	3.77	0.1518	2.40
30	2.23	1.24	2.39	0.3534	2.76

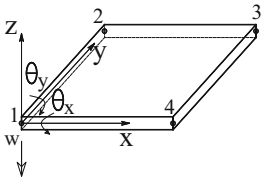

Fig. 2 Plate bending element DOF

The solution goes through an iterative process in calculating the bridge displacement under the vehicle until the increase in the bridge displacement is less than the specified percentage [36]. In the first step, the bridge is assumed to have zero displacements and the vehicle contact force is calculated for the whole simulation time using Eq. 5 (in the first step $f_{\mathrm{vc}_i} = k_{\mathrm{s}} \cdot r_i$). The next step is to calculate the vehicle response by solving Eq. 3 using Newmark-beta integration scheme. The vehicle accelerations are used afterward in Eq. 6 to calculate the applied force on the bridge. The bridge equation of motion is then solved using the same integration scheme to calculate the bridge displacement vector, $\{u_{\mathrm{b}}\}_i$. Finally, the bridge displacements, w_{b_i} are calculated as follows:

$$w_{\mathrm{b}_i} = \{u_{\mathrm{b}}\}_i^{\mathrm{T}} \{N_{\mathrm{b}}\}_i \tag{7}$$

Repeating for all i steps gives the vector $\{w_{\mathrm{b}}\}$ which contains the bridge displacement under the vehicle for all time steps. The process is carried out again with the new w_{b_i} values following the same sequence. This is repeated until the ratio between the maximum bridge displacement in the old and new profiles is less than 1%. The procedure is illustrated in Fig. 3.

4 Apparent profile calculation algorithm

When a vehicle is traveling on a rigid pavement, measured accelerations in the vehicle can be used to back figure the pavement profile. For a vehicle crossing a bridge, the AP is defined as the profile which would have caused the same vehicle accelerations [37]. Here, the AP is calculated by simulating the vehicle crossing over the bridge. For each time step, the vehicle is in equilibrium with the road reaction force applied to the vehicle wheels. Therefore, if the bridge reaction history at the contact point is known, and the vehicle is modeled without a bridge as shown in Fig. 4, application of the road reaction force history at the vehicle wheels will excite it in the same way it was excited by the bridge. The contact node will also move to mimic the profile that produced this force history, which will be the sum of the road roughness heights plus the bridge displacement, or the AP. Therefore, using the vehicle acceleration histories, the road reaction force history is calculated, and the AP is found by applying this force history to the vehicle model.

The instrumented vehicle first crosses over the bridge when it is in a healthy state, as established, for example, from a major inspection. The corresponding AP is calculated to establish the baseline profile. At a later time, when the bridge may have deteriorated, the AP is calculated again. The difference between this and the baseline profile, referred to as the bridge displacement profile difference (BDPD), will be shown to be sensitive to bridge damage.

The road reaction force of the vehicle is equal to the truck gravity weight, plus the inertial forces produced by the acceleration of the vehicle masses. The vehicle gravity weight is removed from the equation since it does not change through the simulation. The truck inertial forces are calculated using the following equation:

$$f_{\mathrm{r}_i} = -[m_{\mathrm{v}}]\{u_{\mathrm{v}}\}_i\langle 1\rangle, \tag{8}$$

where f_{r_i} is the road reaction at step i. The truck is modeled as a quarter car as described before. However, it has one more degree of freedom which is the contact tire node, m_{c} as shown in Fig. 4. The contact node has insignificant mass and is used only to determine the location of the point of contact. Thus the AP can be found by calculating the displacement history of this node. Equation 9 illustrates the modified vehicle model equation of motion, where $[m_{\mathrm{v}}]'$, $[c_{\mathrm{v}}]'$ and $[k_{\mathrm{v}}]'$ are the modified mass, damping and stiffness matrices for the new model. The contact node degree of freedom is denoted by the subscript 'c'. As shown in the equation, the force vector is set to zeros except for the contact node degree of freedom it will equal the road reaction force f_{r_i} at step i. The vehicle model is solved using the Newmark-beta integration scheme to calculate the contact node displacement history u_{c}, i.e., the AP.

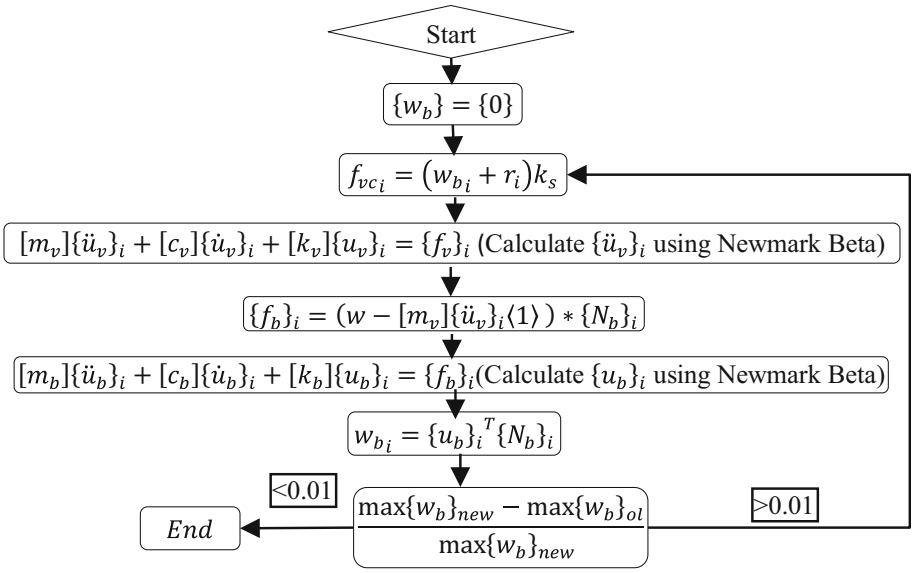

Fig. 3 Vehicle–bridge interaction algorithm

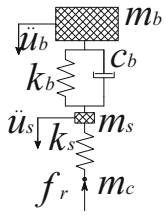

Fig. 4 Apparent profile calculation model

$$[m_v]'\begin{Bmatrix}\{u_v\}\\ u_c\end{Bmatrix}_i + [c_v]'\begin{Bmatrix}\{\dot{u}_v\}\\ \dot{u}_c\end{Bmatrix}_i + [k_v]'\begin{Bmatrix}\{\ddot{u}_v\}\\ u_c\end{Bmatrix}_i = \begin{Bmatrix}\{0\}\\ f_r\end{Bmatrix}_i \quad (9)$$

5 Results for 1D bridge models

The BDPD concept is investigated in two steps. First, the vehicle is simulated crossing over the bridge and the acceleration history of the vehicle masses are found. This is then used to represent the 'measured' accelerations from a real truck. The second step is to use this acceleration history to calculate the AP for each run. The APs for each run are subtracted from the baseline profile to get the BDPD.

The quarter car model is simulated crossing over a 100-m approach at 25 m/s to induce a high excitation to the bridge [35, 38, 39], followed by the simply supported bridge. The road profile for the approach and the bridge is generated randomly for a road of roughness class '*A*' [40]. The bridge is modeled using 100 Euler–Bernoulli beam elements. The first simulation uses a healthy bridge to calculate the baseline (healthy) Apparent Profile, $AP^{0\%}$. Damage is then simulated in the bridge. According to Sinha et al. [41], damage is represented as a crack that causes a linearly varying decrease in flexural stiffness in its vicinity. The damage level is represented as a percentage of the overall bridge cross-sectional depth, *H*. Here, '*x*% damage' represents a crack that causes a loss of stiffness corresponding to an *x*% loss of depth at the crack location. The damage is taken to be located at 70% of the bridge span from the start of the bridge, as shown in Fig. 5. The damage level varies from 5% through 50% in increments of 5%. The AP for each damage simulation is calculated and labeled $AP^{x\%}$, corresponding to *x*% damage level. The APs for the 10-m bridge, with different damage levels, are shown in Fig. 6. The profiles show small differences for different damages; therefore, the study switches to investigate the change in the bridge displacement rather than the absolute displacement.

The bridge displacement profile difference (BDPD) equals the difference between damaged apparent profiles and the baseline (healthy) one ($AP^{0\%}$). The BDPDs for the studied bridges are shown in Fig. 7. It can be seen that the BDPD is very sensitive to structural damages, where for 5% damages it shows a considerable variation from the

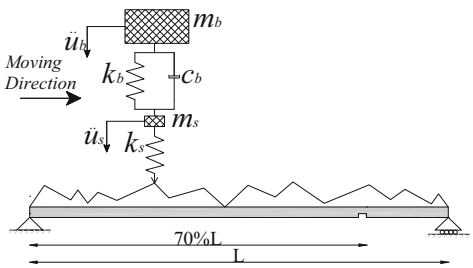

Fig. 5 AP for different damage levels

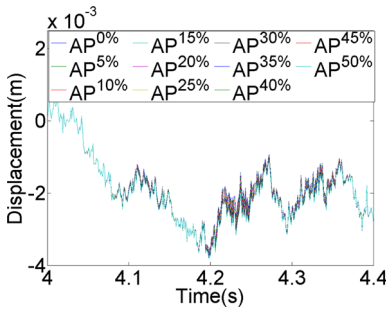

Fig. 6 VBI over a damaged bridge

base line profile. As shown in the figure, the difference increases for higher damage levels which is then can be used for monitoring the level of bridge degradation. In reality, the baseline apparent profile (AP^1) will be measured by passing the vehicle over the bridge under its current structural health status. After a certain period, the bridge will be monitored again with the same vehicle to extract the new apparent profile (AP^2), then the BDPD is calculated by subtraction to indicate the degradation level for the bridge.

6 Results for 2D bridges

In the 1D analyses the crack is implicitly assumed to extend across the full width of the bridge cross section, causing a uniform change in the *EI* values along the bridge width. With the 2D plate bridge model, it is possible to investigate the feasibility of identifying local damage in the bridge. Here the damage is defined by a crack depth and width, which gives a 2D damage representation. In this section, the same linearly varying damage representation is used as before at the same location along the bridge (at 70% *L* from the start), but the damage width is changed. The study considers damage across the whole bridge width, across one-third of the bridge width, and finally across one-tenth of the bridge width. The goal is to investigate the sensitivity of the approach to localized damage in the bridge. The quarter car model crosses over a 100-m approach distance, followed by the bridge, at 25 m/s. The bridge is modeled as a simply supported slab using plate bending elements. The deck is divided into a 10 × 20 mesh of elements. The car travels at a transverse position of 35% *B* from the edge, where *B* is the bridge width as shown in Fig. 8.

First, the damage width is taken as *B,* while the crack depth varies from 0 to 50% in increments of 5%. The quarter car is simulated crossing over the 2D bridges for different damage values. Using the vehicle acceleration histories, the APs for each damage level are back figured as described above. APs are then subtracted from the baseline profile to determine the BDPDs. Figure 9 shows the resulting BDPD curves. Similar to the one-dimensional bridge model, the BDPD shows a high level of sensitivity to structural damages.

The damage width is next reduced to one-third of the bridge span $\left(B/3\right)$, while the damage location and depths are kept the same. Transversely, the damage is located, respectively, at the first, middle and last third, as shown in Fig. 8. The damage depths still vary from 0 to 50% in 5% increments. The process is repeated for the damage width of $\left(B/10\right)$. The results are presented in Fig. 10. The entire process is repeated for 20- and 30-m bridges and they show similar results.

Figure 10 shows that for a local change in stiffness, the approach can still detect a change in BDPD. As can be seen in the figure, the difference is clearer for the last third than for the middle and first thirds. This is because the car is located at 35%*B*, which is close to the last third. Figure 11 shows similar results, this time for the 10-m bridge with a crack of width $\left(B/10\right)$. As illustrated, the algorithm still works, providing BDPD can be measured with sufficient accuracy.

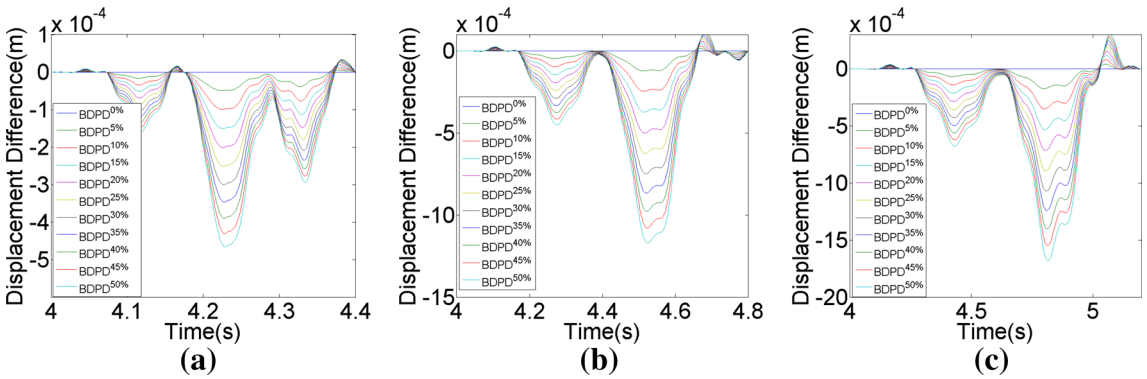

Fig. 7 Bridge displacement profile difference for: **a** 10-m bridge, **b** 20-m bridge, **c** 30-m bridge

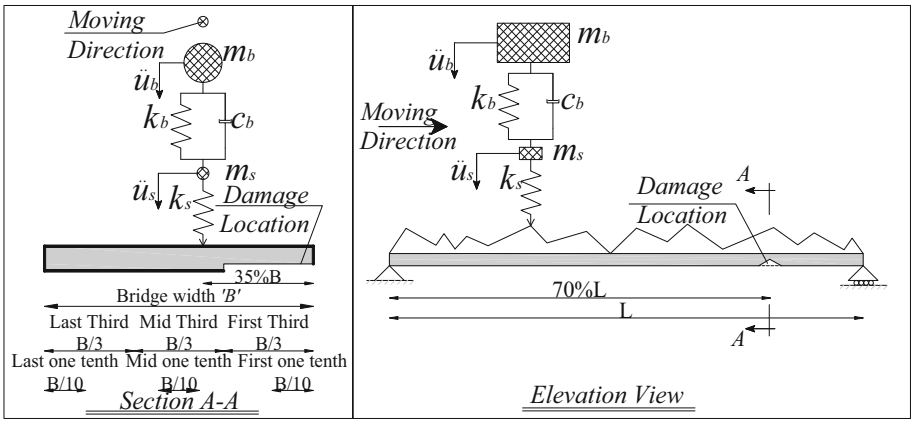

Fig. 8 Damage located at 70% *L* and first one-third bridge width

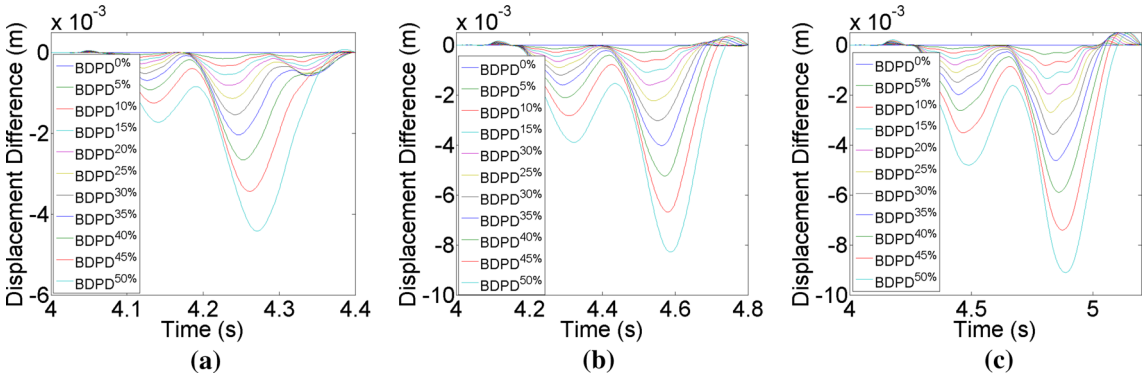

Fig. 9 Bridge displacement profile differences for full-width damage: **a** 10-m bridge, **b** 20-m bridge, **c** 30-m bridge

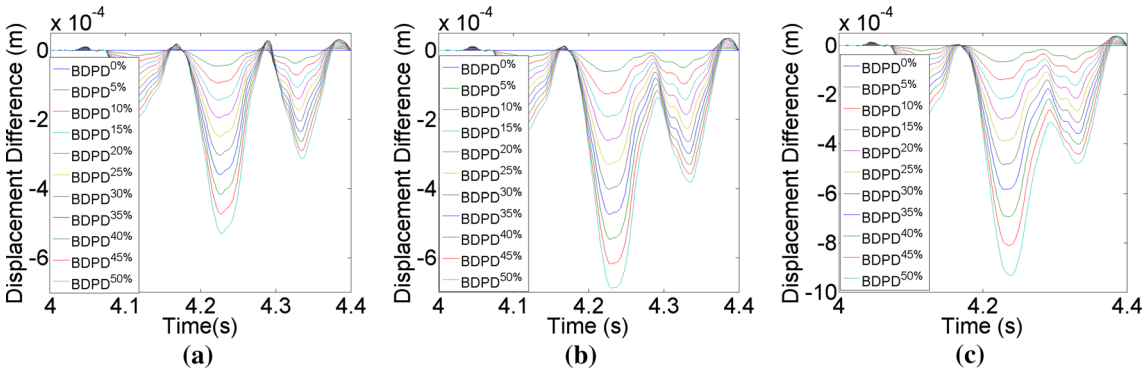

Fig. 10 Bridge displacement profile differences for damage with a width equal to '1/3*B*': **a** first third, **b** mid third, **c** last third

The approach shows a high sensitivity in identifying the damage even for a small damage extent. The proposed approach as illustrated, identifies the change in bridge displacement induced by damage employing the vehicle measurements and by solving the vehicle system only. Therefore, the approach is not a function of the bridge structural status, which makes it suitable for prediction of linear and nonlinear damages. The results shown in this study assumes a linear bridge response under the applied damages (e.g. the exiting damages did not cause a plastic deformation on the structural elements). A further investigation for the attribute of the plastic damages will be investigated in future work.

7 Sensitivity

In this section, the acceleration histories from the vehicle/bridge interaction model are contaminated by random noise to simulate various sources of inaccuracy and the vehicle

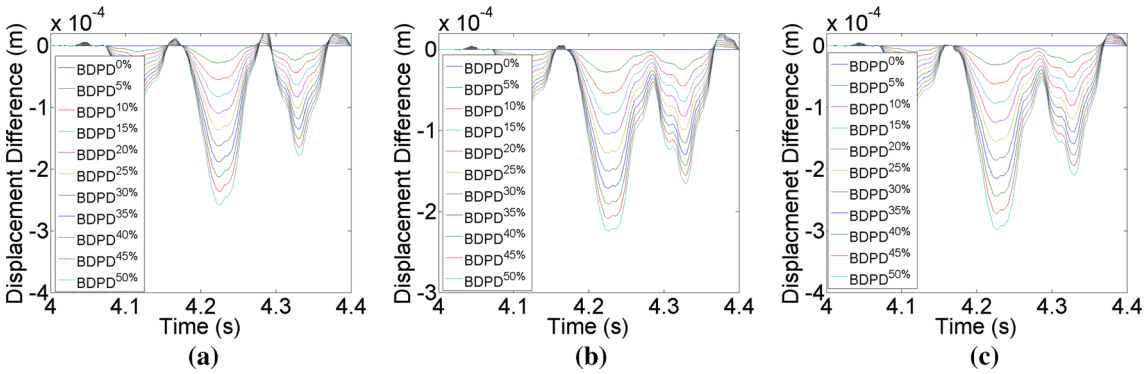

Fig. 11 Bridge displacement profile differences for damage with width equal to '1/10*B*': **a** first one-tenth, **b** mid one-tenth, **c** last one-tenth

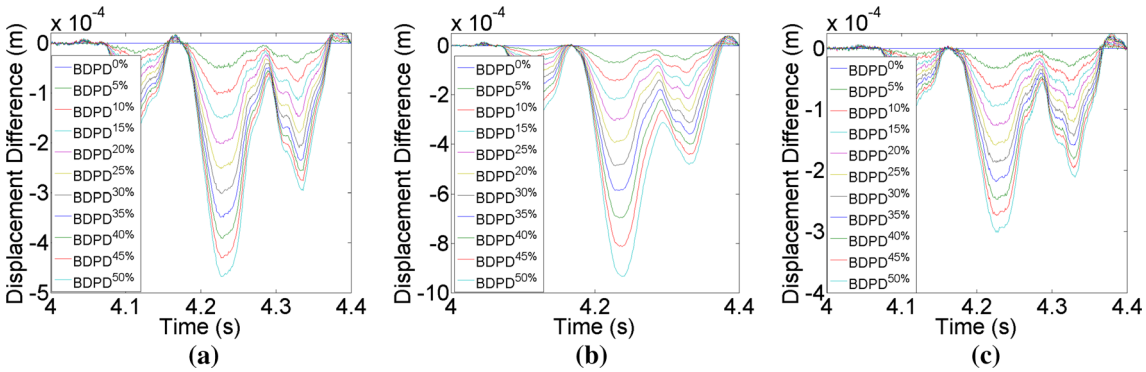

Fig. 12 Bridge displacement profile differences for a contaminated signal: **a** 10-m 1D bridge with, **b** 10-m 2D bridge with damage width equal to '1/30*B*' at first one-third, **c** 10-m 2D bridge with damage width equal to '1/10*B*' at first one tenth

model parameters are assumed to be only known to a certain level of accuracy. Further, it addresses the transverse vehicle position effect on the algorithm.

7.1 Sensitivity to signal noise

To allow for inaccuracy in the acceleration measurements, the signals are contaminated assuming a signal-to-noise ratio (SNR) equal to 60 dB. For the 1D bridge models, the results show a modest vibration around the original BDPDs. Similarly, for the 2D plate bending bridge model, with the same noise level, there is a tiny effect. On the other hand, for the local damage, the BDPDs are affected by the noise level as shown in Fig. 12, and the effect of noise is more pronounced for smaller damage levels.

7.2 Sensitivity to initial conditions

As discussed, the BDPD tracks the increase in the bridge displacement relative to the base line profile. The initial conditions change the absolute magnitude of the APs; however, it does not change the relative increase in bridge displacement due to structural damage. This is because the bridge displacement is only function of the bridge properties. To demonstrate this point, the previous 1D 10-m APs are calculated using zero initial conditions. The APs are shown to be different from Fig. 6 as shown in Fig. 13, while the BDPDs match perfectly with Fig. 7a.

7.3 Sensitivity to truck properties

This section discusses the effect of having a poor theoretical model for the inspection vehicle, which may occur due to inaccurate measuring for the truck properties, or due to error in the calibration process for the real-life truck. In this regard, the truck properties are randomly chosen assuming each property is normally distributed with mean equal to the exact value, and standard deviation equal to 10% of the mean value. The new values for m_s, m_b, k_s, k_b and c_b will create a new inaccurate quarter car model. First, the original (i.e. the correct model) quarter car model will cross the 10-m 1D bridge to generate the acceleration histories. The acceleration will be used as an input to the in-accurate quarter car model to back figure the BDPDs. Figure 14 illustrates the BDPDs for this case, and as shown the algorithm still detects the

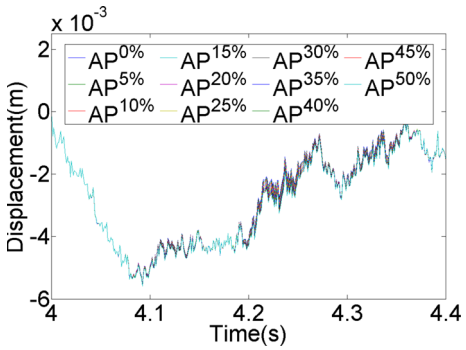

Fig. 13 APs for zero initial conditions

bridge displacement induced by structural damages even using inaccurate vehicle property.

7.4 Sensitivity to vehicle transverse position

The previous findings assume that the vehicle passes on the same track (i.e. the same transverse positions across the bridge), and therefore on the same road profile for each screening, while in reality this is not true. It has been found that for a vehicle passing repetitively through a traffic lane, the transverse position of its wheels can be estimated using statistical models [42]. Blab and Litzka [43] expressed the transverse wheel location using Laplace distribution, where the transverse position is a function of the driving speed and the lane width. For different transverse positions, the vehicle will pass over different profile heights. The profile heights for the new transfer positions can be estimated by interpolation on the road profile carpet. The road profile carpet describes the road profile in planner coordinates, and is generated using ISO-8608 [40] specifications.

In this part, the transverse locations for the quarter car model are changed for each screening (or for each $AP^{x\%}$) using Ronald Balb statistical model. The model parameters are quantified for 90 km/h (25 m/s) driving speed and 360 cm lane width using Ronald Balb charts, and then the probability density function (PDF) for the transverse

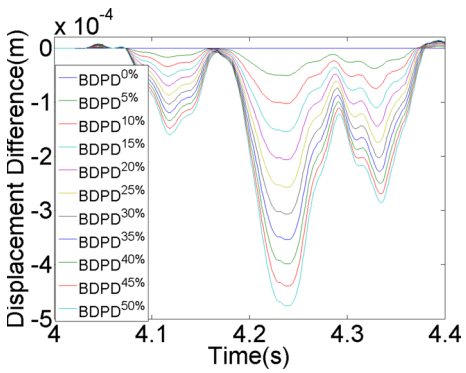

Fig. 14 BDPDs for corrupted truck properties

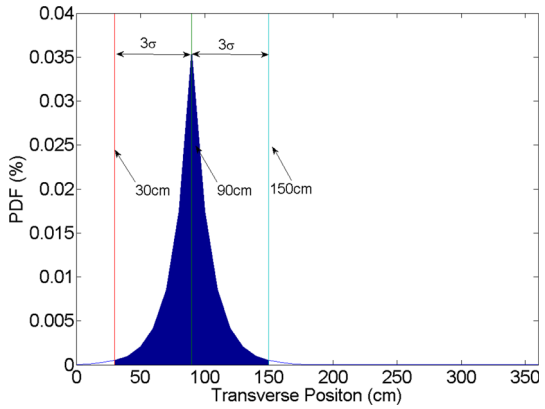

Fig. 15 PDF for transverse position

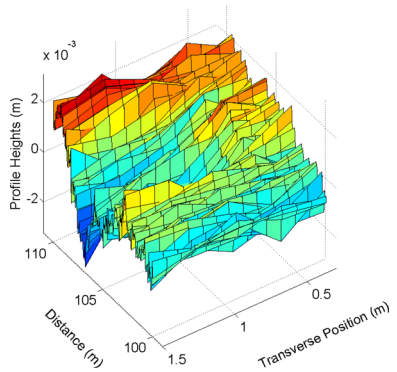

Fig. 16 Carpet profile on the bridge

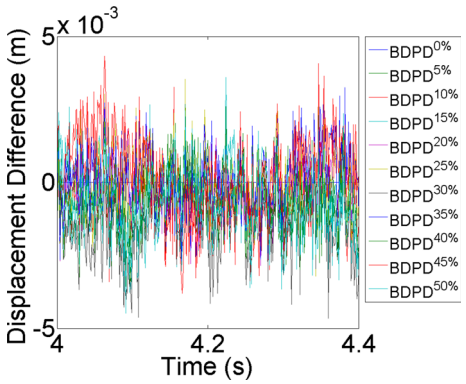

Fig. 17 PDF for transverse position

vehicle position is calculated as shown in Fig. 15. Random values for the PDF are chosen from the shaded area in the figure, which represents a 98.7% probability of occurrence. The corresponding transverse locations are then calculated using the PDF equation. The profile for each transverse position is then calculated via interpolation on the carpet profile which is shown in Fig. 16.

Figure 17 shows the BDPDs for the 10-m 2D bridge considering different transverse vehicle positions. The figure shows that the BDPDs are totally masked by the

differences between road profiles. This happens because the magnitude for the differences between bridge displacements (in other words the BDPDs) are 10^{-4} m as illustrated in the previous figures, while the magnitude for difference between the profiles are 10^{-3} m. This shows that this approach is very sensitive to any changes in the road profile heights, which requires more investigation to eliminate this error.

8 Conclusions

This paper introduces a novel method of monitoring bridges using a non-specialist truck instrumented with accelerometers. The acceleration histories for the axle and body masses are simulated here using a vehicle/bridge interaction model. The accelerations are then used as an input to the Apparent Profile calculation algorithm to calculate the Apparent Profile for each run. In the beginning, the truck passes over the healthy bridge to calculate $AP^{0\%}$ which is used as a baseline against which changes are monitored. In subsequent runs, the acceleration histories are used to find $AP^{x\%}$ which is compared with $AP^{0\%}$ to provide an indication of damage. The difference between $AP^{0\%}$ and $AP^{x\%}$ is the BPPD which is shown to be sensitive to bridge damage.

The approach is tested for 1D and 2D bridge models and successfully responds to small localized changes in bridge stiffness. The approach is used to identify local damage in parts of the cross section of the 2D plate bending bridge model. It is shown to work better when the vehicle passes close to the damage location. The algorithm is found to be insensitive to random signal noise. The study indicates that the algorithm performs well even when the vehicle parameters used are inaccurately known. Finally, the results for different transverse vehicle positions indicate the algorithm sensitivity to road profile heights. Further studies are needed to eliminate this effect.

The approach shows to be robust, and efficient to be used for bridge screening. However, to implement a departure of the approach from the status quo to field application it will require a field test calibration to include the environmental effects and various other uncertainties that may control the approach applicability.

Acknowledgements The authors acknowledge the support provided by the National Science of Foundation of the United States of America (Grant NSF-CMMI-1100742) towards this study.

References

1. FEMA (2007) I-35W bridge collapse and response, Minneapolis, Minnesota, USFA-TR-166
2. Chupanit P, Phromsorn C (2012) The importance of bridge health monitoring. Int Sci Index 6:135–138
3. Enckell M, Glisic B, Myrvoll F, Bergstrand B (2011) Evaluation of a large-scale bridge strain, temperature and crack monitoring with distributed fibre optic sensors. J Civ Struct Health Monit 1(1–2):37–46
4. Kobayashi K, Banthia N (2011) Corrosion detection in reinforced concrete using induction heating and infrared thermography. J Civ Struct Health Monit 1(1–2):25–35
5. Miyamoto A (2013) A new damage detection method for bridge condition assessment in structural health monitoring. J Civ Struct Health Monit 3(4):269–284
6. Quinn W, Angove P, Buckley J, Barrett J, Kelly G (2011) Design and performance analysis of an embedded wireless sensor for monitoring concrete curing and structural health. J Civ Struct Health Monit 1(1–2):47–59
7. Yang Y, Lin C (2005) Vehicle–bridge interaction dynamics and potential applications. J Sound Vib 284(1):205–226
8. Yang Y-B, Lin C, Yau J (2004) Extracting bridge frequencies from the dynamic response of a passing vehicle. J Sound Vib 272(3):471–493
9. Lin C, Yang Y (2005) Use of a passing vehicle to scan the fundamental bridge frequencies: an experimental verification. Eng Struct 27(13):1865–1878
10. Yang Y, Cheng M, Chang K (2013) Frequency variation in vehicle–bridge interaction systems. Int J Struct Stab Dyn 13(02):1350019
11. Chang K, Kim C, Borjigin S (2014) Variability in bridge frequency induced by a parked vehicle. In: Proceedings of the 4th KKCNN symposium on civil engineering, pp 75–79
12. Kim CW, Kawatani M (2009) Challenge for a drive-by bridge inspection. In: International conference; 10th, structural safety and reliability; safety, reliability and risk of structures, infrastructures and engineering systems, ICOSSAR2009, Osaka, Japan
13. McGetrick PJ, Gonzlez A, OBrien EJ (2009) Theoretical investigation of the use of a moving vehicle to identify bridge dynamic parameters. Insight-Non-Destruct Test Cond Monit 51(8):433–438
14. Keenahan J, OBrien EJ, McGetrick PJ, Gonzalez A (2014) The use of a dynamic truck-trailer drive-by system to monitor bridge damping. Struct Health Monit 13(2):143–157
15. W-m Li, Z-h Jiang, T-l Wang, H-p Zhu (2014) Optimization method based on generalized pattern search algorithm to identify bridge parameters indirectly by a passing vehicle. J Sound Vib 333(2):364–380
16. Malekjafarian A, OBrien EJ (2014) Application of output only modal method to the monitoring of bridges using an instrumented vehicle. In: Civil engineering research in Ireland
17. Toshinami T, Kawatani M, Kim C (2010) Feasibility investigation for identifying bridge's fundamental frequencies from vehicle vibrations. In: Bridge maintenance, safety, management and life-cycle optimization: Proceedings of the fifth international IABMAS conference, Philadelphia, USA, 11–15 July 2010. CRC Press, p 108
18. Pandey A, Biswas M, Samman M (1991) Damage detection from changes in curvature mode shapes. J Sound Vib 145(2):321–332
19. Zhu X, Law S (2006) Wavelet-based crack identification of bridge beam from operational deflection time history. Int J Solids Struct 43(7):2299–2317
20. Zhang Y, Wang L, Xiang Z (2012) Damage detection by mode shape squares extracted from a passing vehicle. J Sound Vib 331(2):291–307
21. Yang Y, Li Y, Chang K (2014) Constructing the mode shapes of a bridge from a passing vehicle: a theoretical study. Smart Struct Syst 13(5):797–819

22. Malekjafarian A, OBrien EJ (2014) Identification of bridge mode shapes using short time frequency domain decomposition of the responses measured in a passing vehicle. Eng Struct 81:386–397
23. Curadelli R, Riera J, Ambrosini D, Amani M (2008) Damage detection by means of structural damping identification. Eng Struct 30(12):3497–3504
24. González A, OBrien EJ, McGetrick P (2012) Identification of damping in a bridge using a moving instrumented vehicle. J Sound Vib 331(18):4115–4131
25. McGetrick PJ (2012) The use of an instrumented vehicle to monitor transport infrastructure. University College Dublin, Dublin
26. Gonzalez I, Karoumi R (2015) BWIM aided damage detection in bridges using machine learning. J Civ Struct Health Monit 5(5):715–725
27. Zhang Y, Lie ST, Xiang Z (2013) Damage detection method based on operating deflection shape curvature extracted from dynamic response of a passing vehicle. Mech Syst Signal Process 35(1):238–254
28. Miyamoto A, Yabe A (2011) Bridge condition assessment based on vibration responses of passenger vehicle. In: Journal of physics: conference series, vol 1. IOP Publishing, p 012103
29. Miyamoto A, Yabe A (2012) Development of practical health monitoring system for short-and medium-span bridges based on vibration responses of city bus. J Civ Struct Health Monit 2(1):47–63
30. Cebon D (1999) Handbook of vehicle–road interaction. ALWAYS
31. Harris NK, OBrien EJ, González A (2007) Reduction of bridge dynamic amplification through adjustment of vehicle suspension damping. J Sound Vib 302(3):471–485
32. Logan D (2011) A first course in the finite element method. Cengage Learn
33. Zienkiewicz OC, Taylor RL (2000) The finite element method: solid mechanics, vol 2. Butterworth-Heinemann, Oxford
34. Yang Y, Yau J, Wu Y (2004) Vehicle-bridge interaction dynamics. World Scientific, Hackensack, NJ
35. González A (2010) Vehicle-bridge dynamic interaction using finite element modelling. Sciyo, Croatia
36. Clough RW, Penzien J (1975) Dynamics of structures, Monograph
37. OBrien EJ, Keenahan J (2015) Drive-by damage detection in bridges using the apparent profile. Struct Control Health Monit 22(5):813–825
38. González A, OBrien EJ, McGetrick P (2010) Detection of bridge dynamic parameters using an instrumented vehicle. In: 5th World conference on structural control and monitoring, 12–14 July, Tokyo, Japan
39. Malekjafarian A, McGetrick PJ, OBrien EJ (2015) A review of indirect bridge monitoring using passing vehicles. Shock Vib 2015:16. doi:10.1155/2015/286139
40. ISO-8608 (1995) Mechanical vibration-road surface profiles-reporting of measured data. International Organization for Standardization (ISO), Geneva
41. Sinha J, Friswell M, Edwards S (2002) Simplified models for the location of cracks in beam structures using measured vibration data. J Sound Vib 251(1):13–38
42. BLAB R (1995) Die Fahrspurverteilung als Einflussgro6e bei der Bemessung des Strafienoberbaus. Dissertation an der Technischen Universitat Wien, Fakultat fur Bauingenieurwesen, Wien
43. Blab R, Litzka J (1995) Measurements of the lateral distribution of heavy vehicles and its effects on the design of road pavements. In: Proceedings of the international symposium on heavy vehicle weights and dimensions, road transport technology. University of Michigan, pp 389–395